# Indirect Study of the Astrophysically Relevant $^6$Li$(p,\alpha)^3$He Reaction by Means of the Trojan Horse Method

Aurora Tumino,[1,2] Claudio Spitaleri,[1,2] Luciano Pappalardo,[3] Silvio Cherubini,[2,4] Antonio Del Zoppo,[2] Marco La Cognata,[2] Agatino Musumarra,[1,2] Maria Grazia Pellegriti,[1,2] Rosario Gianluca Pizzone,[1,2] Angelo Rinollo,[1,2] Claus Rolfs,[4] Stefano Romano[1,2] and Stefan Typel[5]

[1]*Dipartimento di Metodologie Fisiche e Chimiche per l'Ingegneria, Universitá di Catania, Catania, Italy*
[2]*Laboratori Nazionali del Sud - INFN Catania, Italy*
[3]*Texas A&M University, College Station, Texas, USA*
[4]*Ruhr-Universität, Bochum, Germany*
[5]*Gesellschaft für Schwerionenforschung mbH, Theorie, Darmstadt, Germany*

The Trojan Horse Method was applied to the $^2$H($^6$Li,$\alpha^3$He)$n$ three-body reaction in order to extract the bare nucleus $S(E)$ factor for the $^6$Li$(p,\alpha)^3$He reaction. The three-body reaction was performed in two kinematically complete experiments at beam energies of 25 and 14 MeV. The selected quasi-free coincidence yield was compared with the result of a Monte Carlo calculation where the entering two-body cross section was the result of a $R$-matrix parameterization of the direct two-body cross section. The quite good agreement throughout the investigated region above and below the $p$-$^6$Li Coulomb barrier, allowed for the extraction of the bare $S(E)$ factor in the astrophysical energy region. The $S(0)$ value together with an independent estimate of the screening potential $U_e$ were derived and compared with those obtained from direct measurements.

## §1. Review of the Trojan Horse Method

In recent years the Trojan Horse Method (THM) has been developed and applied to a number of nuclear reactions[1)–8)] in order to extract the behavior of the bare $S(E)$ factor at sub-Coulomb energies, relevant information to astrophysics. The THM replaces the astrophysical $A+x\rightarrow c+C$ two-body reaction by a suitable $A+a\rightarrow c+C+b$ three-body process, establishing a relation between the two reactions by using nuclear reaction theories. The three-body process is chosen in such a way that the involved target $a$ (or equivalently the projectile) has a wave function with a large amplitude for a $x$-$b$ cluster configuration, $x$ being the target (or equivalently the projectile) of the two-body reaction. In a selected part of the three-body phase space where the other cluster $b$ remains spectator to the process, the three-body reaction can be regarded as an off-shell two-body reaction, usually referred to as a quasi-free reaction. Since the three-body process occurs at an energy above the Coulomb barrier, the main feature is the actual suppression of both the Coulomb barrier and the screening effects in the off-shell two-body cross section. Nevertheless the quasi-free $A+x$ process can occur even at very low sub-Coulomb energies thanks to the key role of the $x$-$b$ binding energy in compensating for the $A+a$ relative motion. This is indeed a different approach to the THM compared to the original idea of Ref. 1), where the initial velocity of the projectile $A$ is compensated for by the Fermi motion of $x$. In that

framework a quite large momentum of the order of 200 MeV/$c$ or more is needed. But the relative yield of the experimental momentum distribution at such momenta can be very small, in particular for a $l$=0 inter-cluster motion (for example $p$-$n$ motion inside $^2$H or $\alpha$-$d$ motion inside $^6$Li). This would make very critical the separation from other competitive reaction mechanisms. Moreover, the theoretical description of the tails of the momentum distribution is a hard task, their shape being very sensitive to it. In our approach to the THM the inter-cluster motion is only needed to fix the accessible astrophysical energy region within a chosen cutoff in momentum distribution, usually of the order of few tents of MeV/$c$. In this framework, the so called "quasi-free two-body energy" is given by

$$E_{q.f.} = E_{Ax} - B_{x\text{-}b} \pm E_{xb}, \tag{1·1}$$

where $E_{Ax}$ is the beam energy in the center of mass of the $A + x$ two-body reaction, $B_{x\text{-}b}$ represents the binding energy of the two clusters $x$ and $b$, and $E_{xb}$ is related to the $x$-$b$ intercluster motion. A detailed theoretical formalism has been developed in a post form Distorted-Wave Born description to deduce a relation between the triple differential cross section and the two-body cross section of interest.[9),10)] In order to derive an expression of the three-body $T$-matrix element in terms of the two-body $S$-matrix elements, the surface approximation is applied, i.e. only reactions at the surface of the nuclei are assumed to contribute significantly to the matrix element, the optical potentials being strongly absorptive for small distances between the colliding nuclei. This allows to replace the full scattering wave function by its asymptotic form for radii larger than a cutoff radius $R$, whose value is nearly the sum of the radii of the two colliding nuclei. Furthermore, replacing the distorted waves in the $T$-matrix element with plane waves this leads to a simpler form for the three-body cross section similar to that of the plane-wave impulse approximation.[9),10)] Yet the complete information on the two-body scattering process is retained and, as long as the energies involved are high enough, the introduced approximations do not change the energy dependence of the two-body cross section but only its absolute value. Using the above approximations, the triple differential cross section is given by

$$\frac{d^3\sigma}{dE_C d\Omega_C d\Omega_c} = \mathrm{KF} \left| W(\vec{Q}_{Bb}) \right|^2 \frac{v_{Cc}}{v_{Ax}} \sum_l P_l C_l \frac{d\sigma_l}{d\Omega}(Cc \to Ax), \tag{1·2}$$

where KF is a kinematical factor,[7)] W($\vec{Q}_{Bb}$) is connected to the wave function of the Trojan Horse nucleus $a$ in momentum space, $\frac{d\sigma_l}{d\Omega}$ represents the on-shell two-body cross section for the $C + c \to A + x$ reaction in partial wave $l$, and $P_l$ is the inverse of the penetrability factor,[7)] which compensates for the Coulomb suppression of the on-shell two-body cross section at low energy. Because of the presence of the $C_l$ constant the absolute value of the two-body cross section cannot be deduce. However absolute cross sections can be obtained through normalization to direct data available at higher energies.

## §2. Experimental details

The experimental study of the $^2$H($^6$Li,$\alpha^3$He)$n$ reaction was performed at two different beam energies, 25 and 14 MeV.[7),8)] The first experiment at 25 MeV was performed with the SMP Tandem van de Graaff accelerator at the Laboratori Nazionali del Sud in Catania and the second one at 14 MeV with the 4 MV Tandem accelerator at the Dynamitron Tandem Laboratorium in Bochum. A 200 $\mu$g/cm$^2$ $CD_2$ target was bombarded with a $^6$Li beam, with a spot size on target of about 1 mm diameter. The experimental set-up consisted of two $\Delta E - E$ telescopes with 20 $\mu$m silicon detectors as $\Delta E$- and 1000 $\mu$m Position Sensitive Detectors (PSD) as E-detector. The two telescopes, called T1 and T2 in the following, were placed on opposite sides of the beam direction covering the laboratory angles 14.5° to 24° and 28.3° to 37.7°, respectively, with equal solid angles of 12.5 msr. The wide angular ranges allowed to have several quasi-free ($\theta_\alpha$,$\theta_{^3He}$) angular pairs contributing to the process and momentum values for the undetected neutron spectator ranging from about $-100$ MeV/$c$ to about 100 MeV/$c$. The quasi-free condition $p_n \sim 0$ MeV/$c$ for the break-up process of interest was fulfilled when $\alpha$ and $^3$He were detected and identified in T1 and T2, respectively. The trigger for the event acquisition was given by the coincidence between the hits of the two telescopes. Energy and position signals for the detected particles were processed by standard electronics together with the delay between the time signals for each coincidence event.

## §3. Data analysis and results

In order to identify the channel of interest $\alpha$ and $^3$He loci have been selected in the $\Delta E - E$ two-dimensional plots of the T1 and T2 telescopes, respectively. The kinematics were reconstructed under the assumption of a neutron as third particle, leading to the $Q$-value spectrum shown in Fig. 1. The spectrum shows a sharp peak just below 2 MeV which corresponds to the channel of interest, i.e. $^3$He+$\alpha$+$n$, whose calculated $Q$-value is 1.79 MeV. Besides, a second peak at about 4 MeV is associated with the $^6$Li+$p$ $\rightarrow\alpha$+$^3$He two-body interaction ($Q$-value = 4.018 MeV) due to the contaminant $^1$H ions in the target. The corresponding loci of events in the $E_{^3He}$ vs $E_\alpha$ plane are shown in Fig. 2. The locus associated with the $^3$He+$\alpha$+$n$ three-body channel that was selected for the further analysis, is well separated from the straight line of the two body process.

The resulting spectra make us confident on the quality of the performed calibration, and on the possibility to well identify the $^3$He+$\alpha + n$ channel. In order to check the presence of the quasi-free contribution, the angular correlation analysis was performed on the data, i.e. coincidence spectra were projected on the $E_{^3He}(E_\alpha)$ axis for a fixed angle of one of the two particles, $\theta_{^3He}(\theta_\alpha)$ and varying the other angle within the angular range of the detector. An example of the resulting spectra is shown in Fig. 3. The arrows mark the condition of nearly zero neutron momentum. The feature expected for a quasi-free process shows up, that is, the coincidence yield decreases while moving away from $p_n\sim$zero. This conditions in Fig. 3 corresponds to the ($\theta_{^3He}$,$\theta_\alpha$)=(34.5°,18.8°) angle pair. Similar results have been obtained for

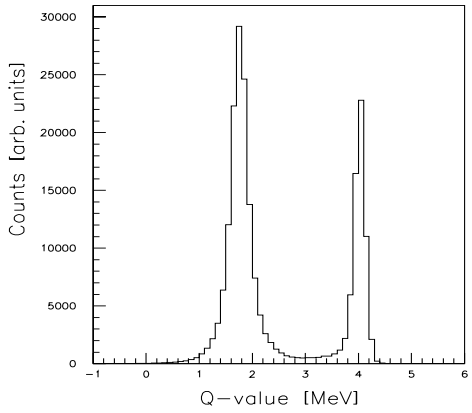


Fig. 1. $Q$-value spectrum for the $\alpha$-$^3$He coincidence events.

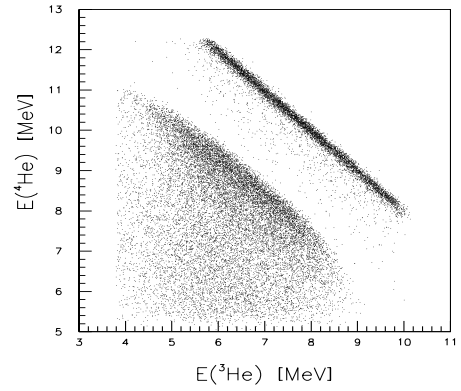


Fig. 2. Kinematical loci corresponding to the $\alpha$-$^3$He coincidence events.

other quasi-free angle pairs. The reconstructed experimental quasi-free momentum distribution for the neutron is reported in Fig. 4 and fairly agrees with the expected theoretical behaviour (dashed line in Fig. 4) that, for a deuteron as Trojan Horse, is given in terms of a Hulthén wave function in momentum space.[5),7)]

In order to select the region where the quasi-free mechanism is dominant, only coincidence events for neutron momenta ranging from $-30$ MeV/$c$ to 30 MeV/$c$ were considered in the further analysis. The three-body experiment was simulated by means of a Monte Carlo calculation based on the theoretical approach previously described. A pure quasi free reaction mechanism was assumed and all experimental constraints in energy and scattering angles for the detected particles were taken into account. The momentum distribution of the neutron inside the deuteron was described in terms of the parameterization given in Ref. 5). The two-body cross section entering the calculation is the result of a single-level $R$-matrix parameterization of the $^6$Li+$p$ reaction,[11)] which accounts for s- and p-waves in the entrance channel. The s-wave contribution describes the low-energy non-resonant part of the cross section and the p-wave is introduced because the $^6$Li+$p$ two-body reaction proceeds also through the $5/2^-$ resonant state of $^7$Be at 7.2 MeV.[11)] The level parameter values for the $R$-matrix fit are given in Table I of Ref. 7). A background resonance at 30 MeV was assumed for all states involved in the $R$-matrix calculation, except for the resonance in the initial p-wave, whose structure was described by the $^2F_{5/2}$ channel in the $^3$He+$^4$He final partition. A channel radius of 4.0 fm was used. The result of the $R$-matrix calculation is shown in Fig. 3. Dashed and dotted lines represent the $l$=0 and $l$=1 contributions to the two-body cross section respectively. Their incoherent sum (full line) is superimposed to the direct data from Ref. 11). Our $R$-matrix fit gives a total $\chi^2 = 5.35$ for the cross section, which is rather good for 30 data points and 13 variable parameters. The fit appears to better reproduce the behaviour of the data in the full range than that of Ref. 11). The selected coincidence yield, still not corrected for the geometric efficiency of the experimental set-up, is shown in Fig. 4

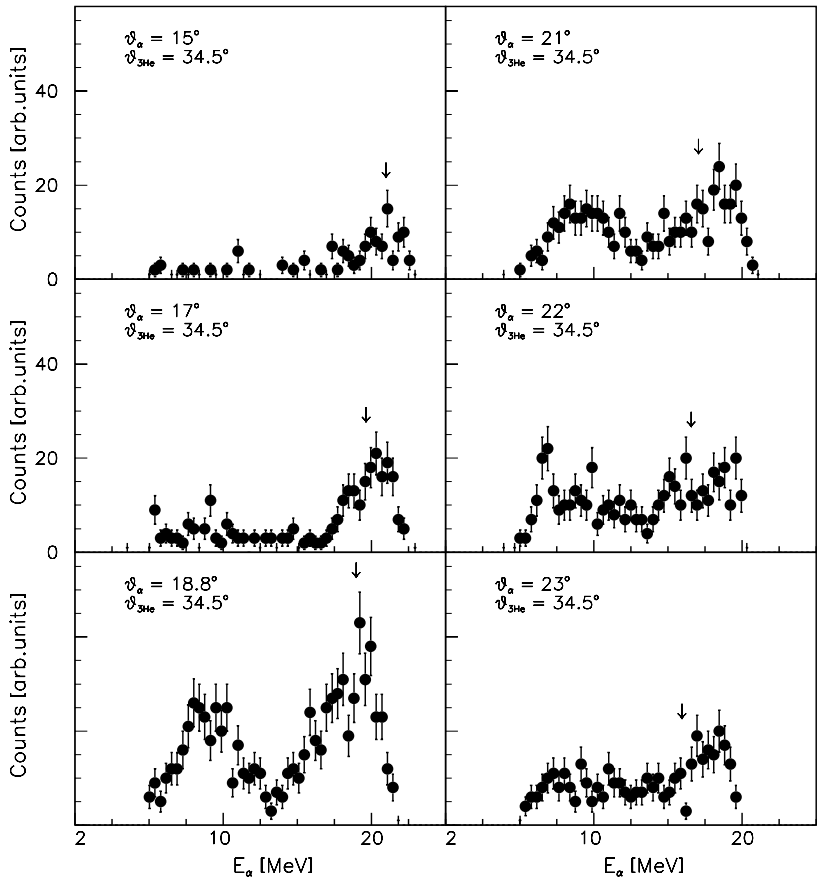


Fig. 3. Angular correlation spectra: $\alpha$-$^3$He coincidence events are projected on the $E_\alpha$-axis for a fixed $\theta_{^3\mathrm{He}}$ and different $\theta_\alpha$ within angular ranges of $\pm 0.5^\circ$. The arrow marks the condition corresponding to $p_n$=0 MeV/$c$.

as a function of the $p$-$^6$Li relative energy.

A wide $p$-$^6$Li relative energy range is populated, from about 2.5 MeV down to astrophysical energies. The three-body cross section from the Monte Carlo calculation is also shown (full line), together with the separate $l$=0 (dashed line) and $l$=1 (dotted line) contributions. The calculation reproduces quite well the experimental behaviour confirming for the first time the validity of the THM above and below the Coulomb barrier in the same experiment. The further step was to extract the bare $S(E)$ factor from the coincidence yield in order to be compared with the direct one. The three-body coincidence yield was then divided by the result of a Monte Carlo simulation assuming a constant on-shell $S(E)$ factor. Penetrability effects, due to the presence of both Coulomb (1.2 MeV) and centrifugal (3.9 MeV) barriers in the direct data, were fully accounted for in the procedure.

The obtained $S(E)$ factor is shown in Fig. 5 (full circles) and compared with the one directly measured (open symbols)[11),12)] in the region below 1 MeV. The nor-

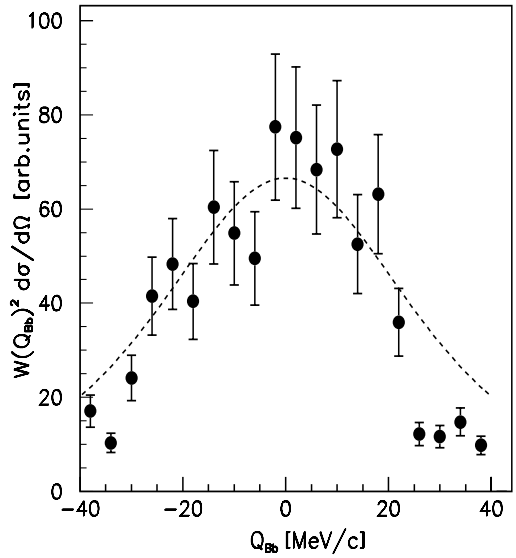


Fig. 4. Experimental momentum distribution for the spectator neutron (full circles), compared with the corresponding theoretical behaviour (dashed line).

malization to the direct data was performed at energy above the Coulomb barrier.[7)]

The overall agreement is quite good in the region above $\sim$ 100 keV, where the electron screening effects on the direct data are still negligible. The disagreement between the two sets of data below this region is indeed attributed to the presence of electron screening effects on the direct ones. The full line superimposed on the indirect data represents the result of a second order polynomial fit to them, $S(E) = 3.00 - 3.02\ E + 1.93\ E^2$, which gives a bare $S(0)$ value of 3.00 $\pm$ 0.19 MeV b. This value agrees within 1% with that reported in the NACRE compilation.[13)] Once deduced the parameterization of the bare $S(E)$ factor, the THM allows for an independent estimate of the screening potential $U_e$.[5)] To this aim the bare $S(E)$ polynomial parameterization given above was multiplied by the known screening enhancement factor $\exp(\pi\eta U_e/E)$[5)] (where $\eta$ is the Sommerfeld parameter). Our $U_e$ estimate is 450 $\pm$ 100 eV and represents the mean value within the region delimited by the other two full lines in Fig. 7, corresponding to $U_e$ values of 350 (lower line) and 550 (upper line) eV. The deduced $U_e$ is in agreement within the experimental errors with that extracted from the extrapolated direct $S(E)$ factor and is affected by a smaller uncertainty. Moreover from the comparison with the $U_e$ estimates from the $^7$Li+$p \rightarrow \alpha$+$\alpha$ and $^6$Li+$d \rightarrow \alpha$+$\alpha$ reactions, the present value confirm the isotopic independence of the screening potential.

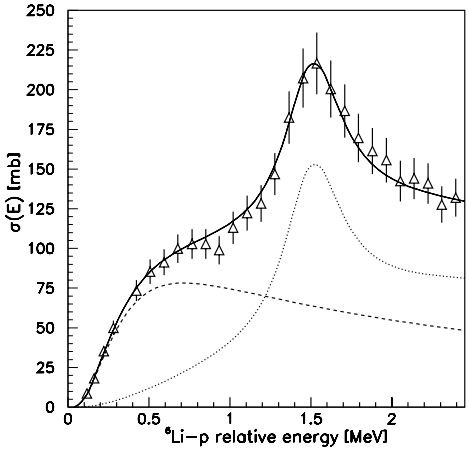


Fig. 5. $R$-matrix fit (full line) to the $^6\mathrm{Li}(p,\alpha)^3\mathrm{He}$ experimental cross section from Ref. 11) (open triangles). Dashed and dotted lines show the separate $l$=0 and $l$=1 contributions.

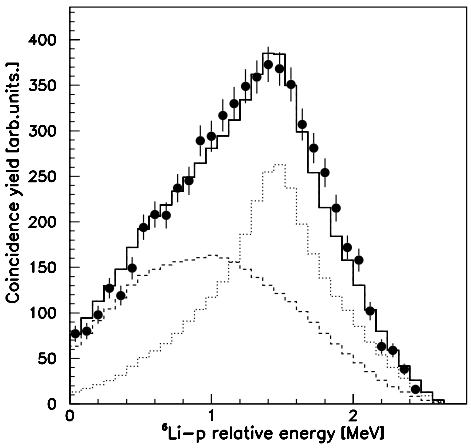


Fig. 6. Quasi free coincidence yield projected onto the $^6$Li-$p$ relative energy (full circles); full line: calculated three-body cross section. Dashed and dotted lines show the separate $l$=0 and $l$=1 contributions.

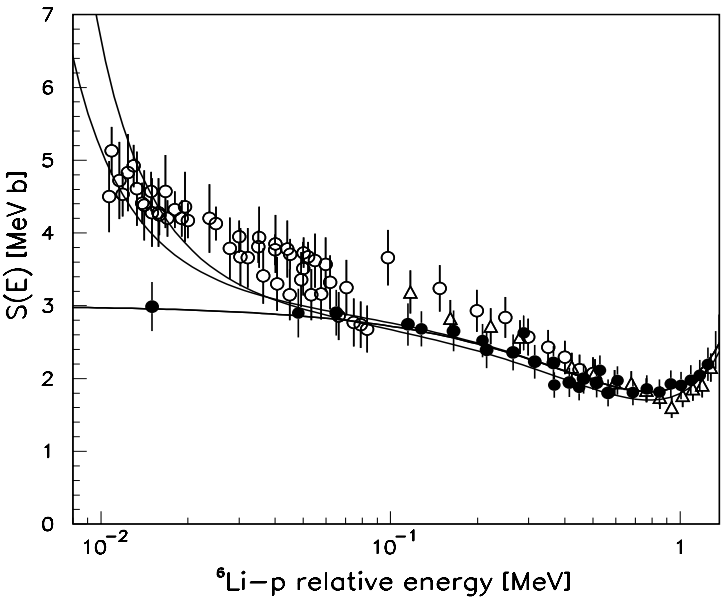


Fig. 7. $S(E)$ factor from indirect data (full circles) reported from 0 to 1 MeV, compared with the direct one (open symbols). The full line represents a second order polynomial fit to the indirect data.

**References**


1) G. Baur, Phys. Lett. B **178** (1986), 135.
2) C. Spitaleri, M. Aliotta, S. Cherubini, M. Lattuada, Dj. Miljanić, S. Romano, N. Soić, M. Zadro and R. A. Zappalà, Phys. Rev. C **60** (1999), 055802.
3) C. Spitaleri, M. Aliotta, P. Figuera, M. Lattuada, R. G. Pizzone, S. Romano, A. Tumino, C. Rolfs, L. Gialanella, F. Strieder, S. Cherubini, A. Musumarra, Dj. Miljanić, S. Typel and H. H. Wolter, Eur. Phys. J. A **7** (2000), 181.
4) C. Spitaleri, S. Typel, R. G. Pizzone, M. Aliotta, S. Blagus, M. Bogovac, S. Cherubini, P. Figuera, M. Lattuada, M. Milin, Dj. Miljanić, A. Musumarra, M. G. Pellegriti, D. Rendić, C. Rolfs, S. Romano, N. Soić, A. Tumino, H. H. Wolter and M. Zadro, Phys. Rev. C **63** (2001), 055801.
5) M. Lattuada, R. G. Pizzone, S. Typel, P. Figuera, Dj. Miljanić, A. Musumarra, M. G. Pellegriti, C. Rolfs, C. Spitaleri and H. H. Wolter, Astrophys. J. **562** (2001), 1076.
6) C. Spitaleri, S. Cherubini, A. Del Zoppo, A. Di Pietro, P. Figuera, M. Gulino, M. Lattuada, Dj. Miljanić, A. Musumarra, M. G. Pellegriti, R. G. Pizzone, C. Rolfs, S. Romano, S. Tudisco and A. Tumino, Nucl. Phys. A **719** (2003), 99.
7) A. Tumino, C. Spitaleri, A. Di Pietro, P. Figuera, M. Lattuada, A. Musumarra, M. G. Pellegriti, R. G. Pizzone, S. Romano, C. Rolfs, S. Tudisco and S. Typel, Phys. Rev. C **67** (2003), 065803.
8) A. Tumino, C. Spitaleri, L. Pappalardo, S. Cherubini, A. Del Zoppo, M. La Cognata, A. Musumarra, M. G. Pellegriti, R. G. Pizzone, A. Rinollo, S. Romano and S. Typel, Nucl. Phys. A **718** (2003), 499.
9) S. Typel and H. Wolter, Few Body Syst. **29** (2000), 75.
10) S. Typel and G. Baur, Ann. of Phys. **305** (2003), 228.
11) A. J. Elwyn, R. E. Holland, C. N. Davids, L. Meyer-Schützmeister, F. P. Mooring and W. Ray Jr., Phys. Rev. C **20** (1997), 1984.
12) S. Engstler, G. Raimann, C. Angulo, U. Greife, C. Rolfs, U. Schröder, E. Somorjai, B. Kirch and K. Langanke, Z. Phys. A **342** (1992), 471.
13) C. Angulo et al., Nucl. Phys. A **656** (1999), 3.